

This discussion paper is/has been under review for the journal Atmospheric Chemistry and Physics (ACP). Please refer to the corresponding final paper in ACP if available.

# The covariation of Northern Hemisphere summertime CO<sub>2</sub> with surface temperature at boreal latitudes

D. Wunch<sup>1</sup>, P. O. Wennberg<sup>1</sup>, J. Messerschmidt<sup>1</sup>, N. Parazoo<sup>2</sup>, G. C. Toon<sup>1,2</sup>,  
N. M. Deutscher<sup>3</sup>, G. Keppel-Aleks<sup>4</sup>, C. M. Roehl<sup>1</sup>, J. T. Randerson<sup>4</sup>, T. Warneke<sup>3</sup>,  
and J. Notholt<sup>3</sup>

<sup>1</sup>California Institute of Technology, Pasadena, CA, USA

<sup>2</sup>Jet Propulsion Laboratory, California Institute of Technology, Pasadena, CA, USA

<sup>3</sup>University of Bremen, Bremen, Germany

<sup>4</sup>Department of Earth System Science, University of California, Irvine, California, USA

Received: 12 March 2013 – Accepted: 10 April 2013 – Published: 19 April 2013

Correspondence to: D. Wunch (dwunch@gps.caltech.edu)

Published by Copernicus Publications on behalf of the European Geosciences Union.

ACPD

13, 10263–10301, 2013

Covariation of X<sub>CO<sub>2</sub></sub>  
with boreal  
temperature

D. Wunch et al.

Title Page

Abstract

Introduction

Conclusions

References

Tables

Figures

◀

▶

◀

▶

Back

Close

Full Screen / Esc

Printer-friendly Version

Interactive Discussion



## Abstract

We observe significant interannual variability in the strength of the seasonal cycle drawdown in northern midlatitudes from measurements of CO<sub>2</sub> made by the Total Carbon Column Observing Network (TCCON) and the Greenhouse Gases Observing Satellite (GOSAT). This variability correlates with surface temperature in the boreal latitudes. The TCCON measurements give an average covariation between the X<sub>CO<sub>2</sub></sub> seasonal cycle minima and boreal surface temperature of  $1.3 \pm 0.7 \text{ ppm K}^{-1}$ . Assimilations from CarbonTracker 2011 and CO<sub>2</sub> simulations using the Simple Biosphere exchange Model (SiB) transported by GEOS-Chem underestimate this covariation. Both atmospheric transport and biospheric activity contribute to the observed covariation.

## 1 Introduction

The global terrestrial ecosystem, the oceans, and fossil fuel burning control the atmospheric concentrations and variability of carbon dioxide (CO<sub>2</sub>). On interannual time scales, variations in the terrestrial biosphere, driven by changes in surface temperature, precipitation, and atmospheric transport, leads to atmospheric variability in CO<sub>2</sub> (Houghton, 2000; Randerson et al., 1997). On these time scales, warm years tend to be associated with more rapid increases in atmospheric CO<sub>2</sub>, and cool years with reduced growth rates (Braswell et al., 1997). This positive relationship between temperature and atmospheric CO<sub>2</sub> is attributed primarily to a strong positive sensitivity of ecosystem respiration ( $R_e$ ) to surface temperature, and concurrently a negative sensitivity of gross primary production (GPP, or photosynthesis) (Doughty and Goulden, 2008).

The shape of the seasonal cycle in atmospheric CO<sub>2</sub> in the northern midlatitudes is primarily determined by the seasonal imbalance between  $R_e$  and GPP (Randerson et al., 1997), which is referred to as net ecosystem exchange (NEE), where positive NEE is defined here as a net flux of CO<sub>2</sub> into the atmosphere. At high latitudes, there

ACPD

13, 10263–10301, 2013

Covariation of X<sub>CO<sub>2</sub></sub> with boreal temperature

D. Wunch et al.

Title Page

Abstract

Introduction

Conclusions

References

Tables

Figures

◀

▶

Back

Close

Full Screen / Esc

Printer-friendly Version

Interactive Discussion



is a significant time lag between GPP and  $R_e$ : GPP peaks around the summer solstice when photosynthesis is at a seasonal maximum, whereas  $R_e$  peaks later in summer when air and ground temperatures are warmest. This creates a negative NEE during the growing season (June, July and August) (Lloyd and Taylor, 1994). The growing season NEE has the largest magnitude over the temperate and boreal forest region of the Northern Hemisphere (Fung et al., 1987), producing the observed seasonal cycle in northern midlatitude CO<sub>2</sub> (Machta, 1972, and Fig. 1). The seasonal cycles at all northern midlatitudes are highly sensitive to changes in the NEE in the boreal forest region (D'Arrigo et al., 1987; Randerson et al., 1997; Keppel-Aleks et al., 2011), where there is also significant temperature-driven variability that changes sign over the course of an annual cycle (Randerson et al., 1999; Piao et al., 2008).

Previous analyses of the role of temperature on atmospheric CO<sub>2</sub> have relied on highly precise and accurate atmospheric CO<sub>2</sub> concentrations or fluxes measured by surface or near-surface in situ instruments located throughout the world. In this paper, we use measurements of column-averaged dry-air mole fractions of CO<sub>2</sub>, denoted X<sub>CO<sub>2</sub></sub>, from the Total Carbon Column Observing Network (TCCON, Wunch et al., 2011a) and from the Greenhouse Gases Observing Satellite (GOSAT, Hamazaki, 2005; Yokota et al., 2009) to examine the interannual variability of the seasonal cycle minimum and its relationship with surface temperature. Compared with surface in situ measurements of CO<sub>2</sub> mole fractions, X<sub>CO<sub>2</sub></sub> is influenced much less by planetary boundary layer height changes, and possesses a much larger spatial sensitivity footprint (on the order of hundreds to thousands of kilometers, Keppel-Aleks et al., 2011). The north-south gradients in X<sub>CO<sub>2</sub></sub> in the Northern Hemisphere summertime are large, and hence the latitudinal origin of the measured air parcel strongly influences its X<sub>CO<sub>2</sub></sub> (Keppel-Aleks et al., 2012).

There have been marked interannual differences in the seasonal cycle minima of X<sub>CO<sub>2</sub></sub> in the Northern Hemisphere in recent years (Figs. 1, 2). Guerlet et al. (2013) have also described significant differences in the 2009 and 2010 seasonal cycle amplitudes using the GOSAT data. These interannual differences are sometimes underestimated

Covariation of X<sub>CO<sub>2</sub></sub> with boreal temperature

D. Wunch et al.

[Title Page](#)

[Abstract](#)

[Introduction](#)

[Conclusions](#)

[References](#)

[Tables](#)

[Figures](#)

◀

▶

◀

▶

[Back](#)

[Close](#)

[Full Screen / Esc](#)

[Printer-friendly Version](#)

[Interactive Discussion](#)



**Covariation of  $X_{CO_2}$  with boreal temperature**

D. Wunch et al.

[Title Page](#)[Abstract](#)[Introduction](#)[Conclusions](#)[References](#)[Tables](#)[Figures](#)[|◀](#)[▶|](#)[◀](#)[▶|](#)[Back](#)[Close](#)[Full Screen / Esc](#)[Printer-friendly Version](#)[Interactive Discussion](#)

in Earth system models, which explicitly represent feedbacks between climate and terrestrial carbon fluxes (Keppel-Aleks et al., 2013).

We find that the measured  $X_{CO_2}$  seasonal cycle minima are correlated with the measured surface temperature anomalies at boreal latitudes. Using atmospheric total column measurements, the CarbonTracker assimilation output (CarbonTracker, 2011) and global  $CO_2$  simulations using the Simple Biosphere model (Sellers et al., 1996a), we investigate the following processes for their contribution to the observed interannual variability in  $X_{CO_2}$ : the relative contributions of fire, fossil fuel, terrestrial biosphere, and ocean fluxes using CarbonTracker, and dynamical drivers of interannual variability using the GEOS-Chem model.

In the following sections, we describe the data and model sources, and outline our analysis methods. We then discuss the results of the analyses.

## 2 TCCON

The TCCON is composed of ground-based Fourier transform spectrometers distributed throughout the world that provide measurements of  $X_{CO_2}$  (Wunch et al., 2011a). We use data from the four longest-running Northern Hemisphere TCCON sites: Park Falls, Wisconsin, USA ( $46^{\circ}$  N,  $90^{\circ}$  W, Washenfelder et al., 2006), Lamont, Oklahoma, USA ( $37^{\circ}$  N,  $97^{\circ}$  W), Białystok, Poland ( $53^{\circ}$  N,  $23^{\circ}$  E, Messerschmidt et al., 2012a), and Bremen, Germany ( $53^{\circ}$  N,  $9^{\circ}$  E). In Bremen, the construction of the solar tracker was completed in 2006, so we include measurements from the beginning of the subsequent calendar year. The  $X_{CO_2}$  from these four sites have been calibrated to the World Meteorological Office scale through comparisons with aircraft profiles (Wunch et al., 2010; Messerschmidt et al., 2011). We use the GGG2012 version of the TCCON data, available from <http://tcccon.ipac.caltech.edu>.

### 3 GOSAT

The GOSAT satellite, carrying the Thermal and Near-Infrared Sensor for carbon Observation Fourier transform spectrometer (TANSO-FTS), was launched in January 2009 and has a ground-repeat cycle of 3 days and a footprint size of approximately  $100 \text{ km}^2$

- 5 ([Yokota et al., 2009](#); [Crisp et al., 2012](#)). We use the  $X_{\text{CO}_2}$  derived from GOSAT spectra by the Atmospheric CO<sub>2</sub> Observations from Space (ACOS) build 2.9 retrieval algorithm (Crisp et al., 2012; O'Dell et al., 2012). Data from 5 April 2009 through 19 April 2011 are used in this study. (At the time this paper was written, interferograms recorded between 19 April 2011 through the summer of 2011 were transformed into spectra using
- 10 an algorithm that is known to produce unreliable results, and so we do not use those data.) Following the methodology of Wunch et al. (2011b), biases in the ACOS-GOSAT  $X_{\text{CO}_2}$  introduced by the retrieval algorithm are reduced by minimizing the variability in the measurements in the Southern Hemisphere. The parameters used to minimize variability are listed in Table 1.

- 15 We define GOSAT-TCCON coincidences in the same manner as Wunch et al. (2011b). We use relatively wide latitude ( $\pm 10^\circ$ ), longitude ( $\pm 30^\circ$ ) and time criteria ( $\pm 5$  days), but restrict the GOSAT measurements to those having a free-tropospheric temperature within  $\pm 2$  K of that measured over the TCCON station. This allows averaging of measurements of air with similar dynamical origin. All GOSAT data that satisfy these
- 20 criteria for a given day are averaged.

### 4 CarbonTracker

CarbonTracker release 2011 ([Peters et al., 2007](#), <http://carbontracker.noaa.gov/>; henceforth CT2011) is an ensemble data assimilation scheme that uses surface, tower, and ship-borne in situ measurements of atmospheric CO<sub>2</sub> and the TM5 atmospheric transport model to produce 4-D fields of CO<sub>2</sub> (CarbonTracker, 2011). The TM5 model ([Krol et al., 2005](#)) is driven by the European Centre for Medium-range Weather

[Title Page](#)[Abstract](#)[Introduction](#)[Conclusions](#)[References](#)[Tables](#)[Figures](#)[|◀](#)[▶|](#)[◀](#)[▶](#)[Back](#)[Close](#)[Full Screen / Esc](#)[Printer-friendly Version](#)[Interactive Discussion](#)

Forecast (ECMWF) assimilated winds (Uppala et al., 2005; Molteni et al., 1996). There are four CO<sub>2</sub> flux “modules” embedded within CT2011: one for each of fire, fossil fuel, terrestrial biosphere, and ocean. These fluxes add to a background field to produce variability in assimilated CO<sub>2</sub>. There are two priors for each of the fossil fuel, biosphere, and ocean flux modules, resulting in eight separate inversions, and the ensemble mean is reported as the result.

Only the terrestrial biosphere and ocean modules are optimized in the assimilation scheme: as with most assimilation schemes, the fire and fossil fuel fields are prescribed. The fire emissions are prescribed using the Global Fire Emissions Database (GFEDv3, CarbonTracker, 2011; Giglio et al., 2006; van der Werf et al., 2010; Mu et al., 2011). CT2011 assumes that the fossil fuel emissions are known from reported annual national and global inventories compiled by the Carbon Dioxide Information Analysis Center (CDIAC, Boden et al., 2011; CarbonTracker, 2011).

The terrestrial biosphere module in CT2011 is optimized based on priors from the monthly mean Carnegie-Ames-Stanford Approach (CASA) balanced ecosystem exchange model (Potter et al., 1993; Randerson et al., 1997), which uses satellite measurements of the normalized difference vegetation index (NDVI) and fractional photosynthetically active radiation (fPAR) as proxies for plant phenology, and year-specific weather. Diurnal and synoptic variability in  $R_e$  is imposed through a  $Q_{10}$  relationship with surface air temperatures ( $R_e \propto Q_{10}^{(T-T_0)/10}$ ), assuming a  $Q_{10}$  of 1.5 for respiration globally (CarbonTracker, 2011).

The ocean module optimizes prior fluxes provided by oceanic flux inversions (Jacobson et al., 2007), and measurements of partial pressure CO<sub>2</sub> in the ocean surface (Takahashi et al., 2009). The prior fluxes have a smooth trend, but no interannual variability. Any interannual variability in the optimized fluxes from the oceanic module of CT2011 is due to atmospheric surface winds interacting with the ocean surface, affecting the gas transfer efficiency. The magnitude of the interannual variability is small compared with the biosphere (CarbonTracker, 2011).

Covariation of X<sub>CO<sub>2</sub></sub> with boreal temperature

D. Wunch et al.

[Title Page](#)

[Abstract](#)

[Introduction](#)

[Conclusions](#)

[References](#)

[Tables](#)

[Figures](#)

◀

▶

◀

▶

[Back](#)

[Close](#)

[Full Screen / Esc](#)

[Printer-friendly Version](#)

[Interactive Discussion](#)



**Covariation of  $X_{CO_2}$  with boreal temperature**

D. Wunch et al.

[Title Page](#)[Abstract](#)[Introduction](#)[Conclusions](#)[References](#)[Tables](#)[Figures](#)[|◀](#)[▶|](#)[◀](#)[▶|](#)[Back](#)[Close](#)[Full Screen / Esc](#)[Printer-friendly Version](#)[Interactive Discussion](#)

We use CT2011 output sampled at the locations of the TCCON stations in this study. We smooth the  $CO_2$  profiles with the TCCON column averaging kernels and a priori profiles, using the Rodgers and Connor (2003) method, and integrate the smoothed profiles to produce daily  $CTX_{CO_2}$ . (Note that to compute total columns from the  $CO_2$  profiles associated with the individual flux modules, we simply integrate the  $CO_2$  profiles to produce  $CTX_{CO_2}^{module}$ .)

## 5 GEOS-Chem and SiB

GEOS-Chem is a global chemical transport model with  $CO_2$  simulations described by Suntharalingam et al. (2003, 2004) and updated by Nassar et al. (2010). Typically, the CASA ecosystem exchange model is used to generate a priori biospheric  $CO_2$  fluxes in GEOS-Chem. Messerschmidt et al. (2012b) have recently shown that replacing CASA with the Simple Biosphere model (SiB3, Baker et al., 2008; Sellers et al., 1996a; Parazoo et al., 2008) significantly improves the  $CO_2$  seasonal cycle amplitude and phase compared with TCCON observations. SiB3 calculates year-dependent fluxes using satellite measurements of plant phenology (Sellers et al., 1996b) yielding significant interannual variability in GPP (Baker et al., 2010). Here, phenological parameters are prescribed from the Moderate Resolution Imaging Spectroradiometer (MODIS, Zhao et al., 2006). Ecosystem respiration in SiB is driven by the  $Q_{10}$  relationship with surface air temperature ( $T$ ), modified by a soil moisture term,  $g(m)$  (Denning et al., 1996):

$$R_e = R_0 Q_{10}^{(T-298)/10} g(m) \quad (1)$$

The soil moisture term is defined in Denning et al. (1996, Eq. 8) and is related to the fraction of root zone soil porosity holding water, prescribed for each soil type by Raich et al. (1991). Based on the work of Raich and Schlesinger (1992),  $Q_{10}$  in SiB is set to 2.4.

Here, the GEOS-Chem model was run twice: once with SiB 2009 fluxes (referred to as “SiB 2009”), and once with year-dependent SiB fluxes (referred to simply as “SiB”).

CO<sub>2</sub> profiles from the model are interpolated to the locations of the TCCON stations, smoothed with the TCCON column averaging kernels and a priori profiles, integrated, and then averaged to produce daily SiBX<sub>CO<sub>2</sub></sub>.

## 6 Methods

- 5 To determine the seasonal cycle minimum date and value, we fit the measured X<sub>CO<sub>2</sub></sub> and the CTX<sub>CO<sub>2</sub></sub> time series with an annual periodic function superimposed on the Earth System Research Laboratory (ESRL) global annual CO<sub>2</sub> growth rate (Table 2, Conway and Tans, 2013). We do not assume the ESRL global annual growth rates for the GEOS-Chem time series; instead, we add an additional linear increase term ( $\alpha x$ )  
10 to the fit. The fitted curves do not permit inter-annual variations in the seasonal cycle *shape*. The functional form of the fitted curve is a Fourier series:

$$f(x) = \sum_{k=0}^2 a_k \cos(2\pi kx) + b_k \sin(2\pi kx) \quad (2)$$

where  $x$  is the fractional year (e.g. 2009.62). The coefficients calculated for each time series are in Table 3. The date of the seasonal cycle minimum for each data set is set by the local minimum in the fitted curves. Figure 1 shows the time series at Park Falls, Lamont, Białystok and Bremen measured by the TCCON instruments. Overlaid are the fitted curves for each time series. Figure 2 shows the time series detrended using the ESRL global annual growth rates, marking the date of the seasonal cycle minimum with symbols.

- 15 20 To assess how well the models compare with the TCCON data, we follow Yang et al. (2007) and use a least squares fit to find the amplitude and phase that minimizes differences between the seasonal cycles computed from the models and the TCCON data. Figure 3 shows the detrended seasonal cycles from the fitted curves (i.e. the  $k = 1, 2$  terms from Eq. 2) to the models and the data. The agreement is generally good:

[Title Page](#)

[Abstract](#)

[Introduction](#)

[Conclusions](#)

[References](#)

[Tables](#)

[Figures](#)

◀

▶

◀

▶

[Back](#)

[Close](#)

[Full Screen / Esc](#)

[Printer-friendly Version](#)

[Interactive Discussion](#)



the amplitudes of the SiBX<sub>CO<sub>2</sub></sub> seasonal cycles are too large by ~10–20%, but show good agreement in the timing of the seasonal cycle (within 7 days). The amplitudes and time lags from the CTX<sub>CO<sub>2</sub></sub> seasonal cycles match the TCCON data well, with the exception of a 9 day time lag at Lamont (Table 4).

The seasonal cycle minimum value (which we will call the “drawdown value”) is determined by subtracting the fitted curves from the time series, and averaging the resulting  $\Delta X_{CO_2}$  within ±15 days of the seasonal cycle minimum. The reported errors on the drawdown value represent the standard deviation ( $1\sigma$ ) of the measurements. In years with fewer than 3 days of measurements near the seasonal cycle minimum, this averaging date range is extended to be within ±25 days (Białystok and Bremen data in 2010). The errors for these data points are tripled to reflect the additional uncertainty.

To investigate the impact of the individual CT2011 modules (fires, fossil fuels, terrestrial biosphere, ocean) on the CTX<sub>CO<sub>2</sub></sub> interannual variability, the fitting method described above (Eq. (2)) is not used, because the ESRL growth rate is only applicable to the total CO<sub>2</sub>, and there may be no periodicity to some of the individual components. The  $\Delta CTX_{CO_2}^{module}$  anomalies are instead computed by subtracting a yearly  $\Delta CTX_{CO_2}^{module}$  mean that has been linearly interpolated to each time step. The drawdown values are the averages of these anomalies within ±15 days of the seasonal cycle minimum in total CTX<sub>CO<sub>2</sub></sub>. The standard deviation of those values from year to year is then computed to estimate the interannual variability.

The calculated drawdown values are compared with August surface temperature measurements from the Goddard Institute for Space Science Surface Temperature Analysis (Hansen and Sato, 2004, <http://data.giss.nasa.gov/gistemp/maps/>). We use the 2004–2010 mean temperatures to compute surface temperature anomalies ( $\Delta T$ ) for years 2000–2012. The temperature anomalies are persistent: the July values and patterns are similar to August. Figure 4 shows the 2009 and 2010 August temperature anomalies as examples. As we wish to evaluate the coupling between the X<sub>CO<sub>2</sub></sub> and the CO<sub>2</sub> fluxes, we weight the year-specific surface temperature anomaly by the 2009 integrated growing season respiration from SiB ( $R_e^{2009GS}$ , in kg C m<sup>-2</sup>) between 30–60° N.

## Covariation of X<sub>CO<sub>2</sub></sub> with boreal temperature

D. Wunch et al.

[Title Page](#)

[Abstract](#)

[Introduction](#)

[Conclusions](#)

[References](#)

[Tables](#)

[Figures](#)

◀

▶

[Back](#)

[Close](#)

[Full Screen / Esc](#)

[Printer-friendly Version](#)

[Interactive Discussion](#)



These values are then divided by the 2009 integrated growing season (June, July, and August) ecosystem respiration between 30–60° N to compute a respiration-weighted temperature anomaly,  $\delta T$ , for each year  $y$ . This weights the temperature anomalies more strongly in locations where the biosphere is active, and de-weights regions in which the biosphere is less active (i.e. over barren or snow-covered areas).

$$\delta T_y = \frac{\sum_{j=180^\circ \text{W}}^{180^\circ \text{E}} \sum_{i=30^\circ \text{N}}^{60^\circ \text{N}} R_{eij}^{\text{2009GS}} \Delta T_{ij}^y \Delta a_{ij}}{\sum_{j=180^\circ \text{W}}^{180^\circ \text{E}} \sum_{i=30^\circ \text{N}}^{60^\circ \text{N}} R_{eij}^{\text{2009GS}} \Delta a_{ij}} \quad (3)$$

where  $i$  is the latitude,  $j$  is the longitude,  $\Delta a_{ij}$  is the grid area (in  $\text{m}^2$ ). The value  $\delta T$  has units of temperature (K).

## 7 Results and discussion

Figure 2 shows the detrended  $X_{\text{CO}_2}$ , revealing clear interannual differences in the  $X_{\text{CO}_2}$  seasonal cycle minima that occur in late summer to early autumn. The sites show similar patterns: 2007 and 2010 have relatively weak drawdowns, whereas 2008 and 2009 have relatively strong drawdowns. Surface temperature anomalies show that years 2007 and 2010 have relatively warm summertime mid latitudes, and 2008 and 2009 relatively cool.

The correlation between the drawdown value and respiration-weighted temperature anomaly for the four TCCON data sets is plotted in Fig. 5 and the slopes ( $\frac{\partial \Delta X_{\text{CO}_2}}{\partial \delta T}$ ) are listed in Table 5. The slope of the relationship between the drawdown value and temperature anomaly for Park Falls, Białystok, Bremen and Lamont are consistent within their standard errors, giving a weighted average of  $1.3 \pm 0.7 \text{ ppm K}^{-1}$ . The Bremen slope is significantly smaller than the other slopes, possibly indicating a different relationship

with surface temperatures that could be caused by Bremen's proximity to urban fossil fuel emissions, or its meteorological location. Excluding Bremen from the weighted mean results in an average of  $1.5 \pm 0.8 \text{ ppm K}^{-1}$ . The Białystok slope is consistent with the Park Falls and Lamont slopes, but due to low data yields during the summertimes of 2010 and 2012, the error in the estimated slope is large. The standard errors are generally large at all sites because there is significant day-to-day variability in  $X_{\text{CO}_2}$  near the seasonal cycle minimum due to the influence of synoptic-scale activity on the measured  $X_{\text{CO}_2}$  (Keppel-Aleks et al., 2012). Figure 6 illustrates this increased summertime synoptic-scale "noise". In the summertime, air that has originated from the north (cooler air) tends to have lower  $X_{\text{CO}_2}$  values, whereas air that originated from the south (warmer air) has higher  $X_{\text{CO}_2}$  values, giving rise to high variability in  $X_{\text{CO}_2}$  in the growing season. Covariations between the drawdown values and 30–60° N surface temperatures (not weighted by  $R_e$ ) show larger relative errors on the slopes, but consistent slope values (within error).

It is not robust to compute covariations from the ACOS-GOSAT retrievals over these four locations for only two years, but the  $\Delta X_{\text{CO}_2}$  values from GOSAT agree with the TCCON values well within the errors for 2009 and 2010. More revealing is the spatial distribution of the GOSAT  $\Delta X_{\text{CO}_2} - \delta T$  ratios between 2009 and 2010 (Fig. 7). The spatial pattern is mostly uniform, except near the oceans. This is consistent with our understanding that  $X_{\text{CO}_2}$  has a very large spatial footprint that is essentially hemispheric on seasonal time scales. The cause of this spatial variability near the coasts is unclear.

The significant correlation of  $X_{\text{CO}_2}$  with temperature could point to a large-scale dynamical effect, fires, fossil fuel use, or a biospheric reaction to the temperature changes. It is unlikely to be related to oceanic fluxes, as the interannual variability in  $\text{CO}_2$  from ocean fluxes is negligible (Table 6). The possible effects and an estimate of their relative importance are discussed in turn below.

Covariation of  $X_{\text{CO}_2}$  with boreal temperature

D. Wunch et al.

[Title Page](#)

[Abstract](#)

[Introduction](#)

[Conclusions](#)

[References](#)

[Tables](#)

[Figures](#)

◀

▶

◀

▶

[Back](#)

[Close](#)

[Full Screen / Esc](#)

[Printer-friendly Version](#)

[Interactive Discussion](#)



## 7.1 Dynamics

Variability in the dynamical mixing of CO<sub>2</sub> within and between the mid latitudes and the tropics is expected to be correlated with surface temperature changes, since the meridional thermal structure both responds to and drives north-south transport of air

5 (Trenberth, 1990; Webster, 1981). Therefore, it is plausible that the slopes seen in the TCCON and GOSAT data are influenced by interannual variability in the atmospheric mixing. To test this, we use the GEOS-Chem dynamical fields with static SiB 2009 biogenic fluxes, holding the NEE cycle constant from year to year. The results are shown in the bottom right panel of Fig. 5 and in Table 5. The SiB run with 2009 fluxes shows

10 a weakly positive slope that is ~ 40 % ( $\pm 40 \%$ ) of that observed, indicating that variability in the mixing does contribute to the observed interannual variability in X<sub>CO<sub>2</sub></sub> minima. Because the covariations are computed with column-averaged CO<sub>2</sub>, which is less influenced by local dynamics, this suggests that large-scale dynamics are important: warm years are associated with enhanced poleward transport of high CO<sub>2</sub> air from the subtropics and/or reduced equatorward transport of low CO<sub>2</sub> air from the Arctic, and the

15 converse for cool years.

## 7.2 Fires

High temperature (and lower humidity) conditions might be expected to be correlated with wild fire activity (e.g. Westerling et al., 2006) and therefore increased atmospheric

20 CO<sub>2</sub> (Zhao and Running, 2010). To investigate whether variations in fires have a significant effect on the variations in X<sub>CO<sub>2</sub></sub> seasonal cycle minima, we analyze TCCON measurements of X<sub>CO</sub>, a fire tracer measured simultaneously with the X<sub>CO<sub>2</sub></sub>. The anomalies in X<sub>CO</sub> are calculated in an identical manner to X<sub>CO<sub>2</sub></sub>, except that we do not use the ESRL CO<sub>2</sub> mean growth rate, but fit an additional linear increase parameter ( $\alpha_x$ ). Following Akagi et al. (2011), we assume that the modified combustion efficiency of producing CO<sub>2</sub> from biomass burning is ~ 88 % in the boreal forest, and we convert the measured  $\Delta X_{CO}$  at the time of the X<sub>CO<sub>2</sub></sub> drawdown into the  $\Delta X_{CO_2}$  contribution from

[Title Page](#)[Abstract](#)[Introduction](#)[Conclusions](#)[References](#)[Tables](#)[Figures](#)[◀](#)[▶](#)[Back](#)[Close](#)[Full Screen / Esc](#)[Printer-friendly Version](#)[Interactive Discussion](#)

fires. We show the relationship between  $\Delta X_{\text{CO}_2}$  caused by fires with the respiration-weighted temperature anomaly in Fig. 8. The variability in  $\Delta X_{\text{CO}_2}$  caused by fires is at most  $\sim 0.05 \text{ ppm K}^{-1}$ . Although CO is not a conserved tracer (its oxidation by OH leads to a lifetime of  $\sim 1\text{--}2$  months (Yurganov et al., 2004)), the small slope, even if a lower bound, suggests that fire does not contribute significantly to the observed  $\sim 1.3 \text{ ppm K}^{-1}$  variability.

Consistently, the CT2011 fire signature ( $\text{CTX}_{\text{CO}_2}^{\text{fires}}$ ) accounts for only 6–13 % of the total interannual variability in summertime drawdown  $\text{CTX}_{\text{CO}_2}$  in CarbonTracker (see Table 6). The fire anomalies ( $\Delta \text{CTX}_{\text{CO}_2}^{\text{fires}}$ ) have a weak relationship with the respiration-weighted temperature anomalies (Fig. 8), and a maximum slope of  $\sim 0.05 \text{ ppm K}^{-1}$ .

### 7.3 Fossil fuel

The fossil fuel contribution ( $\text{CTX}_{\text{CO}_2}^{\text{ff}}$ ) to the  $\text{CTX}_{\text{CO}_2}$  contains significant interannual variability ( $\sim 23\%$  in Lamont, Bremen and Białystok, and  $\sim 10\%$  in Park Falls, see Table 6). Because we detrend the TCCON data and CT2011 assimilation output of total  $X_{\text{CO}_2}$  by the annual measured  $\text{CO}_2$  growth rate, much of the variability in the annual fossil fuel emissions will be removed from the  $\Delta X_{\text{CO}_2}$  anomalies and will not contribute to the  $\Delta X_{\text{CO}_2} - \delta T$  slope. Any remaining variability attributed to the fossil fuel signature is likely due partially to the dynamical effects described in Sect. 7.1. The CT2011 fossil fuel signal ( $\text{CTX}_{\text{CO}_2}^{\text{ff}}$ ) is not correlated with the respiration-weighted surface temperature (Fig. 8, bottom panel).

### 7.4 NEE

The most significant contribution to interannual variability in  $\text{CTX}_{\text{CO}_2}$  is the terrestrial biosphere component, which accounts for 60 % in Bremen, increasing to 82 % in Park Falls (see Table 6). Respiration is directly influenced by surface temperature, and GPP is indirectly influenced by temperature through soil moisture. In SiB, both ecosystem

[Title Page](#)[Abstract](#)[Introduction](#)[Conclusions](#)[References](#)[Tables](#)[Figures](#)[◀](#)[▶](#)[◀](#)[▶](#)[Back](#)[Close](#)[Full Screen / Esc](#)[Printer-friendly Version](#)[Interactive Discussion](#)

## Covariation of $X_{\text{CO}_2}$ with boreal temperature

D. Wunch et al.

Title Page

Abstract

Introduction

Conclusions

References

Tables

Figures

◀

▶

◀

▶

Back

Close

Full Screen / Esc

Printer-friendly Version

Interactive Discussion



## 8 Summary and future study

Interannual variability in the seasonal cycle minima of column-averaged dry-air mole fractions of CO<sub>2</sub> is correlated with summertime surface temperature anomalies at boreal latitudes. The CarbonTracker 2011 assimilation and GEOS-Chem simulations suggest that this relationship is caused both by dynamical mixing and biospheric activity, in roughly equal proportion. The effects of emissions from fossil fuel combustion and fires appear to be small and uncorrelated with surface temperature. However, CT2011 and the GEOS-Chem driven SiB  $\Delta X_{\text{CO}_2} - \delta T$  relationships are generally weaker than observed.

It is clear that there are several avenues worth pursuing to further investigate the  $\Delta X_{\text{CO}_2} - \delta T$  relationship. It is important to try other realizations of the dynamics: using different transport models such as TM5, or different underlying wind fields, such as ECMWF or NCEP. Because our results are derived from column-averaged atmospheric CO<sub>2</sub> measurements, which are relatively insensitive to planetary boundary layer (local) dynamics, we anticipate that differences in the large-scale dynamics will dominate the variability.

To further disentangle the effects of NEE on the observed variability, both the effects of GPP and  $R_e$  should be probed. Although interannual variability in GPP is not correlated with  $\delta T$  in SiB, Guerlet et al. (2013) have attributed the interannual variability in the GOSAT 2009–2010 seasonal cycles to reduced carbon uptake (GPP) through their inversions. However, the 2010 Northern Hemisphere had exceptional warming, causing record-breaking heatwaves throughout eastern Europe and Russia, and fires in western Russia (Barriopedro et al., 2011). The correlation between  $\delta T$  and GPP should be explored in other biospheric models, and by using chlorophyll fluorescence (e.g. Frankenberg et al., 2011) instead of, or in conjunction with, the current proxies for plant phenology (e.g. NDVI). Further, the sensitivity of  $R_e$  to temperature ( $Q_{10}$ ) and moisture should be studied further.

<a href="#">Title Page</a>	
<a href="#">Abstract</a>	<a href="#">Introduction</a>
<a href="#">Conclusions</a>	<a href="#">References</a>
<a href="#">Tables</a>	<a href="#">Figures</a>
<a href="#"></a>	<a href="#"></a>
<a href="#"></a>	<a href="#"></a>
<a href="#">Back</a>	<a href="#">Close</a>
<a href="#">Full Screen / Esc</a>	
<a href="#">Printer-friendly Version</a>	
<a href="#">Interactive Discussion</a>	



Developing robust metrics for respiration and GPP responses to temperature is critical for reducing uncertainties in Earth system models and for diagnosing the vulnerability of permafrost carbon pools to future change.

**Acknowledgements.** CarbonTracker 2011 results were provided by NOAA ESRL, Boulder, Colorado, USA from the website at <http://carbontracker.noaa.gov>. US funding for TCCON comes from NASA's Carbon Cycle Program, grant number NNX11AG01G, the Orbiting Carbon Observatory Program, and the DOE/ARM Program. We acknowledge financial support of the Białystok TCCON site from the Senate of Bremen and EU projects IMECC and GEOmon as well as maintenance and logistical work provided by AeroMeteo Service. POW and JTR receive support from NASA's Carbon Cycle Science program (NNX10AT83G). The GOSAT  $X_{CO_2}$  data were obtained from the Atmospheric CO<sub>2</sub> Observations from Space (ACOS) project. We thank the Japanese three parties (NIES, JAXA, MOE) for making the GOSAT spectra available to the scientific community. Self-calibrated PDSI data with Penman-Monteith PE were downloaded from <http://www.cgd.ucar.edu/cas/catalog/climind/pdsi.html>.

## References

- Akagi, S. K., Yokelson, R. J., Wiedinmyer, C., Alvarado, M. J., Reid, J. S., Karl, T., Crounse, J. D., and Wennberg, P. O.: Emission factors for open and domestic biomass burning for use in atmospheric models, *Atmos. Chem. Phys.*, 11, 4039–4072, doi:10.5194/acp-11-4039-2011, 2011. 10274
- Baker, I. T., Prihodko, L., Denning, A. S., Goulden, M., Miller, S., and da Rocha, H. R.: Seasonal drought stress in the Amazon: reconciling models and observations, *J. Geophys. Res.*, 113, G00B01, doi:10.1029/2007JG000644, 2008. 10269
- Baker, I. T., Denning, A. S., and Stöckli, R.: North American gross primary productivity: regional characterization and interannual variability, *Tellus B*, 62, 533–549, doi:10.1111/j.1600-0889.2010.00492.x, 2010. 10269
- Barriopedro, D., Fischer, E. M., Luterbacher, J., Trigo, R. M., and García-Herrera, R.: The hot summer of 2010: redrawing the temperature record map of Europe, *Science*, 332, 220–224, doi:10.1126/science.1201224, 2011. 10277
- Boden, T. A., Marland, G., and Andres, R. J.: Global, Regional, and National Fossil-Fuel CO<sub>2</sub> Emissions, doi:10.3334/CDIAC/00001\_V2011, Carbon Dioxide Information Analysis Center,



Braswell, B. H., Schimel, D. S., Linder, E., and Moore, B.: The response of global  
5 terrestrial ecosystems to interannual temperature variability, *Science*, 278, 870–873,  
doi:10.1126/science.278.5339.870, 1997. 10264

CarbonTracker: Documentation – CT2011, Tech. rep., Earth System Research Laboratory –  
National Oceanic and Atmospheric Administration, available at: [http://www.esrl.noaa.gov/gmd/ccgg/carbontracker/documentation\\_obs.html](http://www.esrl.noaa.gov/gmd/ccgg/carbontracker/documentation_obs.html), 2011. 10266, 10267, 10268

Conway, T. and Tans, P.: Annual mean global carbon dioxide growth rates, available at: <http://www.esrl.noaa.gov/gmd/ccgg/trends/global.html>, NOAA/ESRL, last access: 7 January 2013.  
10 10270

Crisp, D., Fisher, B. M., O'Dell, C., Frankenberg, C., Basilio, R., Bösch, H., Brown, L. R., Cas-  
tano, R., Connor, B., Deutscher, N. M., Eldering, A., Griffith, D., Gunson, M., Kuze, A., Man-  
drake, L., McDuffie, J., Messerschmidt, J., Miller, C. E., Morino, I., Natraj, V., Notholt, J.,  
15 O'Brien, D. M., Oyafuso, F., Polonsky, I., Robinson, J., Salawitch, R., Sherlock, V., Smyth, M.,  
Suto, H., Taylor, T. E., Thompson, D. R., Wennberg, P. O., Wunch, D., and Yung, Y. L.: The  
ACOS CO<sub>2</sub> retrieval algorithm – Part II: Global X<sub>CO<sub>2</sub></sub> data characterization, *Atmos. Meas.  
Tech.*, 5, 687–707, doi:10.5194/amt-5-687-2012, 2012. 10267

Dai, A.: Characteristics and trends in various forms of the Palmer Drought Severity Index during  
20 1900–2008, *J. Geophys. Res.*, 116, D12115, doi:10.1029/2010JD015541, 2011a. 10276

Dai, A.: Drought under global warming: a review, *Wiley Interdisciplinary Reviews, Climate  
Change*, 2, 45–65, doi:10.1002/wcc.81, 2011b. 10276

Dai, A., Trenberth, K. E., and Qian, T.: A global dataset of Palmer Drought Severity Index for  
25 1870–2002: relationship with soil moisture and effects of surface warming, *J. Hydrometeorol.*,  
5, 1117–1130, doi:10.1175/JHM-386.1, 2004. 10276

D'Arrigo, R., Jacoby, G. C., and Fung, I. Y.: Boreal forests and atmosphere-biosphere exchange  
of carbon dioxide, *Nature*, 329, 321–323, doi:10.1038/329321a0, 1987. 10265

Denning, A. S., Collatz, G. J., Zhang, C., Randall, D. A., Berry, J. A., Sellers, P. J., Colello, G. D.,  
30 and Dazlich, D. A.: Simulations of terrestrial carbon metabolism and atmospheric CO<sub>2</sub>  
in a general circulation model, Part 1: Surface carbon fluxes, *Tellus B*, 48, 521–542,  
doi:10.1034/j.1600-0889.1996.t01-2-00009.x, 1996. 10269, 10276

Doughty, C. E. and Goulden, M. L.: Are tropical forests near a high temperature threshold?, *J.  
Geophys. Res.*, 113, G00B07, doi:10.1029/2007JG000632, 2008. 10264

Covariation of X<sub>CO<sub>2</sub></sub>  
with boreal  
temperature

D. Wunch et al.

Title Page

Abstract

Introduction

Conclusions

References

Tables

Figures



Back

Close

Full Screen / Esc

Printer-friendly Version

Interactive Discussion



**Covariation of  $X_{CO_2}$  with boreal temperature**

D. Wunch et al.

[Title Page](#)[Abstract](#)[Introduction](#)[Conclusions](#)[References](#)[Tables](#)[Figures](#)[|](#)[|](#)[◀](#)[▶](#)[Back](#)[Close](#)[Full Screen / Esc](#)[Printer-friendly Version](#)[Interactive Discussion](#)

Frankenberg, C., Fisher, J. B., Worden, J., Badgley, G., Saatchi, S. S., Lee, J.-E., Toon, G. C., Butz, A., Jung, M., Kuze, A., and Yokota, T.: New global observations of the terrestrial carbon cycle from GOSAT: patterns of plant fluorescence with gross primary productivity, *Geophys. Res. Lett.*, 38, 1–6, doi:10.1029/2011GL048738, 2011. 10277

5 Fung, I. Y., Tucker, C. J., and Prentice, K. C.: Application of advanced very high resolution radiometer vegetation index to study atmosphere–biosphere exchange of  $CO_2$ , *J. Geophys. Res.*, 92, 2999–3015, doi:10.1029/JD092iD03p02999, 1987. 10265

Giglio, L., van der Werf, G. R., Randerson, J. T., Collatz, G. J., and Kasibhatla, P.: Global estimation of burned area using MODIS active fire observations, *Atmos. Chem. Phys.*, 6, 957–974, doi:10.5194/acp-6-957-2006, 2006. 10268

10 Guerlet, S., Basu, S., Butz, A., Krol, M., Hahne, P., Houweling, S., Hasekamp, O. P., and Aben, I.: Reduced carbon uptake during the 2010 Northern Hemisphere summer as observed from GOSAT, *Geophys. Res. Lett.*, in press, doi:10.1002/grl.50402, 2013. 10265, 10277

15 Hamazaki, T.: Fourier transform spectrometer for Greenhouse Gases Observing Satellite (GOSAT), *P. SPIE Is. & T. Elect.*, 5659, 73–80, doi:10.1117/12.581198, 2005. 10265

Hansen, J. and Sato, M.: Greenhouse gas growth rates., *P. Natl. Acad. Sci. USA*, 101, 16109–16114, doi:10.1073/pnas.0406982101, 2004. 10271

20 Houghton, R. A.: Interannual variability in the global carbon cycle, *J. Geophys. Res.*, 105, 20121–20130, doi:10.1029/2000JD900041, 2000. 10264

Jacobson, A. R., Mikaloff Fletcher, S. E., Gruber, N., Sarmiento, J. L., and Gloor, M.: A joint atmosphere-ocean inversion for surface fluxes of carbon dioxide: 1. Methods and global-scale fluxes, *Global Biogeochem. Cy.*, 21, GB1019, doi:10.1029/2005GB002556, 2007. 10268

25 Keppel-Aleks, G., Wennberg, P. O., and Schneider, T.: Sources of variations in total column carbon dioxide, *Atmos. Chem. Phys.*, 11, 3581–3593, doi:10.5194/acp-11-3581-2011, 2011. 10265

Keppel-Aleks, G., Wennberg, P. O., Washenfelder, R. A., Wunch, D., Schneider, T., Toon, G. C., Andres, R. J., Blavier, J.-F., Connor, B., Davis, K. J., Desai, A. R., Messerschmidt, J., Notholt, J., Roehl, C. M., Sherlock, V., Stephens, B. B., Vay, S. A., and Wofsy, S. C.: The imprint of surface fluxes and transport on variations in total column carbon dioxide, *Biogeosciences*, 9, 875–891, doi:10.5194/bg-9-875-2012, 2012. 10265, 10273

## Covariation of $X_{CO_2}$ with boreal temperature

D. Wunch et al.

Title Page

Abstract

Introduction

Conclusions

References

Tables

Figures

◀

▶

◀

▶

Back

Close

Full Screen / Esc

Printer-friendly Version

Interactive Discussion



Keppel-Aleks, G., Randerson, J. T., Lindsay, K., Stephens, B. B., Moore, J. K., Doney, S. C., Thornton, P. E., Mahowald, N. M., Hoffman, F. M., Sweeney, C., Tans, P. P., Wennberg, P. O., and Wofsy, S. C.: Atmospheric carbon dioxide variability in the Community Earth System Model: evaluation and transient dynamics during the 20th and 21st centuries, *J. Climate*, in press, 2013. 10266

Krol, M., Houweling, S., Bregman, B., van den Broek, M., Segers, A., van Velthoven, P., Peters, W., Dentener, F., and Bergamaschi, P.: The two-way nested global chemistry-transport zoom model TM5: algorithm and applications, *Atmos. Chem. Phys.*, 5, 417–432, doi:10.5194/acp-5-417-2005, 2005. 10267

Lloyd, J. and Taylor, J. A.: On the temperature dependence of soil respiration, *Funct. Ecol.*, 8, 315, doi:10.2307/2389824, 1994. 10268

Machta, L.: Mauna Loa and global trends in air quality, *B. Am. Meteorol. Soc.*, 53, 402–420, doi:10.1175/1520-0477(1972)053<0402:MLAGTI>2.0.CO;2, 1972. 10265

Messerschmidt, J., Geibel, M. C., Blumenstock, T., Chen, H., Deutscher, N. M., Engel, A., Feist, D. G., Gerbig, C., Gisi, M., Hase, F., Katrynski, K., Kolle, O., Lavrič, J. V., Notholt, J., Palm, M., Ramonet, M., Rettinger, M., Schmidt, M., Sussmann, R., Toon, G. C., Truong, F., Warneke, T., Wennberg, P. O., Wunch, D., and Xueref-Remy, I.: Calibration of TCCON column-averaged  $CO_2$ : the first aircraft campaign over European TCCON sites, *Atmos. Chem. Phys.*, 11, 10765–10777, doi:10.5194/acp-11-10765-2011, 2011. 10266

Messerschmidt, J., Chen, H., Deutscher, N. M., Gerbig, C., Grupe, P., Katrynski, K., Koch, F.-T., Lavrič, J. V., Notholt, J., Rödenbeck, C., Ruhe, W., Warneke, T., and Weinzierl, C.: Automated ground-based remote sensing measurements of greenhouse gases at the Białystok site in comparison with collocated in situ measurements and model data, *Atmos. Chem. Phys.*, 12, 6741–6755, doi:10.5194/acp-12-6741-2012, 2012a. 10266

Messerschmidt, J., Parazoo, N., Deutscher, N. M., Roehl, C., Warneke, T., Wennberg, P. O., and Wunch, D.: Evaluation of atmosphere-biosphere exchange estimations with TCCON measurements, *Atmos. Chem. Phys. Discuss.*, 12, 12759–12800, doi:10.5194/acpd-12-12759-2012, 2012b. 10269

Molteni, F., Buizza, R., Palmer, T. N., and Petroliagis, T.: The ECMWF ensemble prediction system: methodology and validation, *Q. J. Roy. Meteor. Soc.*, 122, 73–119, doi:10.1002/qj.49712252905, 1996. 10268

Mu, M., Randerson, J. T., van der Werf, G. R., Giglio, L., Kasibhatla, P., Morton, D., Collatz, G. J., DeFries, R. S., Hyer, E. J., Prins, E. M., Griffith, D. W. T., Wunch, D., Toon, G. C., Sherlock, V.,

## Covariation of $X_{CO_2}$ with boreal temperature

D. Wunch et al.

Title Page

## Abstract

## Introduction

## Conclusions

## References

Tables

## Figures

1

▶

Page

Class

Full Screen / Esc

[Printer-friendly Version](#)

Interactive Discussion



- Raich, J. W., Rastetter, E. B., Melillo, J. M., Kicklighter, D. W., Steudler, P. A., Peterson, B. J., Grace, A. L., III, B. M., and Vorosmarty, C. J.: Potential net primary productivity in South America: application of a global model, *Ecol. Appl.*, 1, 399, doi:10.2307/1941899, 1991. 10269, 10276
- 5 Randerson, J. T., Thompson, M. V., Conway, T. J., Fung, I. Y., and Field, C. B.: The contribution of terrestrial sources and sinks to trends in the seasonal cycle of atmospheric carbon dioxide, *Global Biogeochem. Cy.*, 11, 535–560, doi:10.1029/97GB02268, 1997. 10264, 10265, 10268
- 10 Randerson, J. T., Field, C. B., Fung, I. Y., and Tans, P. P.: Increases in early season ecosystem uptake explain recent changes in the seasonal cycle of atmospheric CO<sub>2</sub> at high northern latitudes, *Geophys. Res. Lett.*, 26, 2765, doi:10.1029/1999GL900500, 1999. 10265
- Rodgers, C. D. and Connor, B. J.: Intercomparison of remote sounding instruments, *J. Geophys. Res.*, 108, 4116, doi:10.1029/2002JD002299, 2003. 10269
- Sellers, P., Randall, D., Collatz, G., Berry, J., Field, C., Dazlich, D., Zhang, C., Collelo, G., and Bounoua, L.: A revised land surface parameterization (SiB2) for atmospheric GCMS, Part I: Model formulation, *J. Climate*, 9, 676–705, doi:10.1175/1520-0442(1996)009<0676:ARLSPF>2.0.CO;2, 1996a. 10266, 10269
- 15 Sellers, P. J., Tucker, C. J., Collatz, G. J., Los, S. O., Justice, C. O., Dazlich, D. A., and Randall, D. A.: A revised land surface parameterization (SiB2) for atmospheric GCMS, Part II: The generation of global fields of terrestrial biophysical parameters from satellite data, *J. Climate*, 9, 706–737, doi:10.1175/1520-0442(1996)009<0706:ARLSPF>2.0.CO;2, 1996b. 10269
- 20 Suntharalingam, P., Spivakovsky, C. M., Logan, J. A., and McElroy, M. B.: Estimating the distribution of terrestrial CO<sub>2</sub> sources and sinks from atmospheric measurements: sensitivity to configuration of the observation network, *J. Geophys. Res.*, 108, 4452, doi:10.1029/2002JD002207, 2003. 10269
- 25 Suntharalingam, P., Jacob, D. J., Palmer, P. I., Logan, J. A., Yantosca, R. M., Xiao, Y., Evans, M. J., Streets, D. G., Vay, S. L., and Sachse, G. W.: Improved quantification of Chinese carbon fluxes using CO<sub>2</sub>/CO correlations in Asian outflow, *J. Geophys. Res.*, 109, D18S18, doi:10.1029/2003JD004362, 2004. 10269
- 30 Takahashi, T., Sutherland, S. C., Wanninkhof, R., Sweeney, C., Feely, R. a., Chipman, D. W., Hales, B., Friederich, G., Chavez, F., Sabine, C., Watson, A., Bakker, D. C., Schuster, U., Metzl, N., Yoshikawa-Inoue, H., Ishii, M., Midorikawa, T., Nojiri, Y., Körtzinger, A., Steinhoff, T., Hoppema, M., Olafsson, J., Arnarson, T. S., Tilbrook, B., Johannessen, T., Olsen, A., Bellerby, R., Wong, C., Delille, B., Bates, N., and de Baar, H. J.: Climatological mean and

Covariation of X<sub>CO<sub>2</sub></sub> with boreal temperature

D. Wunch et al.

[Title Page](#)

[Abstract](#)

[Introduction](#)

[Conclusions](#)

[References](#)

[Tables](#)

[Figures](#)

[◀](#)

[▶](#)

[◀](#)

[▶](#)

[Back](#)

[Close](#)

[Full Screen / Esc](#)

[Printer-friendly Version](#)

[Interactive Discussion](#)



**Covariation of  $X_{CO_2}$  with boreal temperature**

D. Wunch et al.

[Title Page](#)[Abstract](#)[Introduction](#)[Conclusions](#)[References](#)[Tables](#)[Figures](#)[◀](#)[▶](#)[◀](#)[▶](#)[Back](#)[Close](#)[Full Screen / Esc](#)[Printer-friendly Version](#)[Interactive Discussion](#)

## Covariation of $X_{CO_2}$ with boreal temperature

D. Wunch et al.

[Title Page](#)

[Abstract](#)

[Introduction](#)

[Conclusions](#)

[References](#)

[Tables](#)

[Figures](#)

[◀](#)

[▶](#)

[Back](#)

[Close](#)

[Full Screen / Esc](#)

[Printer-friendly Version](#)

[Interactive Discussion](#)



Westerling, A. L., Hidalgo, H. G., Cayan, D. R., and Swetnam, T. W.: Warming and earlier spring increase western US forest wildfire activity, *Science*, 313, 940–943, doi:10.1126/science.1128834, 2006. 10274

5 Wunch, D., Toon, G. C., Wennberg, P. O., Wofsy, S. C., Stephens, B. B., Fischer, M. L., Uchino, O., Abshire, J. B., Bernath, P., Biraud, S. C., Blavier, J.-F. L., Boone, C., Bowman, K. P., Browell, E. V., Campos, T., Connor, B. J., Daube, B. C., Deutscher, N. M., Diao, M., Elkins, J. W., Gerbig, C., Gottlieb, E., Griffith, D. W. T., Hurst, D. F., Jiménez, R., Keppel-Aleks, G., Kort, E. A., Macatangay, R., Machida, T., Matsueda, H., Moore, F., Morino, I., Park, S., Robinson, J., Roehl, C. M., Sawa, Y., Sherlock, V., Sweeney, C., Tanaka, T., and Zondlo, M. A.: Calibration of the Total Carbon Column Observing Network using aircraft profile data, *Atmos. Meas. Tech.*, 3, 1351–1362, doi:10.5194/amt-3-1351-2010, 2010. 10266

10 Wunch, D., Toon, G. C., Blavier, J.-F. L., Washenfelder, R. A., Notholt, J., Connor, B. J., Griffith, D. W. T., Sherlock, V., and Wennberg, P. O.: The total carbon column observing network, *Philos. T. R. Soc. A*, 369, 2087–2112, doi:10.1098/rsta.2010.0240, 2011a. 10265, 10266

15 Wunch, D., Wennberg, P. O., Toon, G. C., Connor, B. J., Fisher, B., Osterman, G. B., Frankenberg, C., Mandrake, L., O'Dell, C., Ahonen, P., Biraud, S. C., Castano, R., Cressie, N., Crisp, D., Deutscher, N. M., Eldering, A., Fisher, M. L., Griffith, D. W. T., Gunson, M., Heikkinen, P., Keppel-Aleks, G., Kyrö, E., Lindenmaier, R., Macatangay, R., Mendonca, J., Messerschmidt, J., Miller, C. E., Morino, I., Notholt, J., Oyafuso, F. A., Rettinger, M., Robinson, J., Roehl, C. M., Salawitch, R. J., Sherlock, V., Strong, K., Sussmann, R., Tanaka, T., Thompson, D. R., Uchino, O., Warneke, T., and Wofsy, S. C.: A method for evaluating bias in global measurements of  $CO_2$  total columns from space, *Atmos. Chem. Phys.*, 11, 12317–12337, doi:10.5194/acp-11-12317-2011, 2011b. 10267, 10287

20 Yang, Z., Washenfelder, R. A., Keppel-Aleks, G., Krakauer, N. Y., Randerson, J. T., Tans, P. P., Sweeney, C., and Wennberg, P. O.: New constraints on Northern Hemisphere growing season net flux, *Geophys. Res. Lett.*, 34, L12807, doi:10.1029/2007GL029742, 2007. 10270

25 Yokota, T., Yoshida, Y., Eguchi, N., Ota, Y., Tanaka, T., Watanabe, H., and Maksyutov, S.: Global concentrations of  $CO_2$  and  $CH_4$  retrieved from GOSAT: first preliminary results, *Sola*, 5, 160–163, doi:10.2151/sola.2009-041, 2009. 10265, 10267

30 Yurganov, L. N., Blumenstock, T., Grechko, E. I., Hase, F., Hyer, E. J., Kasischke, E. S., Koike, M., Kondo, Y., Kramer, I., Leung, F.-Y., Mahieu, E., Mellqvist, J., Notholt, J., Novelli, P. C., Rinsland, C. P., Scheel, H. E., Schultz, A., Strandberg, A., Sussmann, R., Tanimoto, H., Velazco, V., Zander, R., and Zhao, Y.: A quantitative assessment of the 1998 carbon

monoxide emission anomaly in the Northern Hemisphere based on total column and surface concentration measurements, *J. Geophys. Res.*, 109, D15305, doi:10.1029/2004JD004559, 2004. 10275

5 Zhao, M. and Running, S. W.: Drought-induced reduction in global terrestrial net primary production from 2000 through 2009, *Science*, 329, 940–943, doi:10.1126/science.1192666, 2010. 10274, 10276

Zhao, M., Running, S. W., and Nemani, R. R.: Sensitivity of Moderate Resolution Imaging Spectroradiometer (MODIS) terrestrial primary production to the accuracy of meteorological reanalyses, *J. Geophys. Res.*, 111, G01002, doi:10.1029/2004JG000004, 2006. 10269

[Title Page](#)

[Abstract](#)

[Introduction](#)

[Conclusions](#)

[References](#)

[Tables](#)

[Figures](#)

◀

▶

[Back](#)

[Close](#)

[Full Screen / Esc](#)

[Printer-friendly Version](#)

[Interactive Discussion](#)



## Covariation of $X_{\text{CO}_2}$ with boreal temperature

D. Wunch et al.

**Table 1.** The parameters used to minimize variability in the Southern Hemisphere, in order to reduce the impact of the ACOS-GOSAT retrieval on the  $X_{\text{CO}_2}$  values. The model used in this case includes a small seasonal cycle in the Southern Hemisphere (i.e. Assumption 1 from Wunch et al., 2011b). The blended albedo parameter is defined as  $(2.4(\text{A-band albedo}) - 1.13(\text{strong CO}_2\text{-band albedo}))$ . The  $\Delta P$  parameter is defined as  $(P_{\text{surface}} - P_{\text{prior}})$ , where  $P_{\text{surface}}$  is the retrieved surface pressure, and  $P_{\text{prior}}$  is the a priori value from ECMWF.

parameter	slope	units
blended albedo	$6.4 \pm 0.2$	$\text{ppm} (\text{unit albedo})^{-1}$
$\Delta P$	$-0.136 \pm 0.006$	$\text{ppm hPa}^{-1}$
A-band albedo	$-10.0 \pm 0.5$	$\text{ppm} (\text{unit albedo})^{-1}$
aerosol optical depth	$-12.7 \pm 1.2$	$\text{ppm} (\text{unit aod})^{-1}$
airmass	$-0.5 \pm 0.1$	$\text{ppm airmass}^{-1}$

- [Title Page](#)
- [Abstract](#) | [Introduction](#)
- [Conclusions](#) | [References](#)
- [Tables](#) | [Figures](#)
- [◀](#) | [▶](#)
- [◀](#) | [▶](#)
- [Back](#) | [Close](#)
- [Full Screen / Esc](#)
- [Printer-friendly Version](#)
- [Interactive Discussion](#)



**Covariation of  $X_{\text{CO}_2}$  with boreal temperature**

D. Wunch et al.

**Table 2.** Mean annual  $\text{CO}_2$  growth rates published on the ESRL-NOAA webpage: <http://www.esrl.noaa.gov/gmd/ccgg/trends/global.html>. The rates and their uncertainties are expressed in  $\text{ppmyr}^{-1}$ .

Year	Growth Rate ( $\alpha$ )	Uncertainty
2000	1.25	0.10
2001	1.80	0.10
2002	2.38	0.07
2003	2.24	0.10
2004	1.61	0.05
2005	2.43	0.07
2006	1.74	0.06
2007	2.10	0.07
2008	1.80	0.05
2009	1.69	0.10
2010	2.41	0.06
2011	1.69	0.09
2012	2.77	0.09

- [Title Page](#)
- [Abstract](#) | [Introduction](#)
- [Conclusions](#) | [References](#)
- [Tables](#) | [Figures](#)
- [◀](#) | [▶](#)
- [◀](#) | [▶](#)
- [Back](#) | [Close](#)
- [Full Screen / Esc](#)
- [Printer-friendly Version](#)
- [Interactive Discussion](#)



## Covariation of $X_{\text{CO}_2}$ with boreal temperature

D. Wunch et al.

[Title Page](#)

[Abstract](#)

[Introduction](#)

[Conclusions](#)

[References](#)

[Tables](#)

[Figures](#)

◀

▶

[Back](#)

[Close](#)

[Full Screen / Esc](#)

[Printer-friendly Version](#)

[Interactive Discussion](#)



**Table 3.** Curve fitting parameters for Eq. (2). The parameters  $\alpha$ ,  $a_0$  represent the linear secular increase:  $\alpha$  is in  $\text{ppmyr}^{-1}$  and  $a_0$  is the y-intercept in ppm. Parameter  $a_1$  (ppm) represents the amplitude of the  $\cos(2\pi x)$  term, and  $b_1$  (ppm) represents the amplitude of the  $\sin(2\pi x)$  term. The  $a_2$  and  $b_2$  parameters are the amplitudes of the  $\cos(4\pi x)$  and  $\sin(4\pi x)$  terms, respectively. The drawdown date (DD) and seasonal cycle maximum date (MD) are the dates of the local minima and maxima of the fitted curves, respectively, in day of the year.

Site	$\alpha$	$a_0$	$a_1$	$a_2$	$b_1$	$b_2$	DD	MD
Park Falls (TCCON)	ESRL (see Table 2)	0.81	1.73	-0.51	3.32	-1.48	230	104
Lamont (TCCON)	ESRL (see Table 2)	1.52	0.11	0.54	2.71	-0.55	262	124
Białystok (TCCON)	ESRL (see Table 2)	0.59	2.32	-0.11	3.21	-1.02	232	87
Bremen (TCCON)	ESRL (see Table 2)	1.37	1.64	0.39	3.62	-0.93	245	98
Park Falls (GOSAT)	ESRL (see Table 2)	0.08	1.51	-1.08	3.63	-1.58	225	103
Lamont (GOSAT)	ESRL (see Table 2)	-0.05	0.67	0.12	2.79	-0.99	245	114
Białystok (GOSAT)	ESRL (see Table 2)	-0.08	2.49	0.08	2.93	-1.81	232	108
Bremen (GOSAT)	ESRL (see Table 2)	-0.34	1.34	-0.01	2.89	-1.57	236	114
Park Falls (SiB)	2.22	-4075.59	2.25	-0.51	4.06	-1.00	231	90
Lamont (SiB)	2.29	-4217.89	0.47	0.35	3.15	-0.39	260	102
Białystok (SiB)	2.44	-4511.29	3.26	-0.25	4.05	-0.69	229	67
Bremen (SiB)	2.27	-4169.57	2.36	-0.15	4.42	-0.90	237	85
Park Falls (SiB 2009)	2.25	-4129.40	2.14	-0.51	4.11	-1.16	232	94
Lamont (SiB 2009)	2.31	-4260.74	0.40	0.40	3.19	-0.39	261	104
Białystok (SiB 2009)	2.40	-4438.20	3.27	-0.10	4.21	-0.72	232	65
Bremen (SiB 2009)	2.29	-4216.98	2.34	-0.07	4.35	-0.97	238	87
Park Falls (CT2011)	ESRL (see Table 2)	0.93	1.39	-0.41	3.09	-1.37	232	106
Lamont (CT2011)	ESRL (see Table 2)	1.33	0.37	0.10	2.32	-0.52	251	108
Białystok (CT2011)	ESRL (see Table 2)	1.13	1.61	-0.18	3.16	-1.03	235	98
Bremen (CT2011)	ESRL (see Table 2)	1.23	1.18	0.04	3.17	-1.10	241	107

**Table 4.** Time lag and amplitude adjustments necessary to best fit the TCCON data with the model fits. The time lag is in days, where a positive time lag means that the model should be delayed to best fit the TCCON data. The amplitude is multiplicative, so a value less than 1 means that the model amplitude should be reduced to best fit the TCCON data. See Fig. 3 for the related figure.

Site	SiB		Carbon Tracker	
	Time Lag	Amplitude	Time Lag	Amplitude
Park Falls	$2.5 \pm 1.4$	$0.86 \pm 0.01$	$-2.30 \pm 1.19$	$1.10 \pm 0.03$
Lamont	$5.9 \pm 2.2$	$0.89 \pm 0.02$	$9.55 \pm 2.07$	$1.17 \pm 0.05$
Bialystok	$6.3 \pm 3.2$	$0.79 \pm 0.03$	$-5.96 \pm 2.69$	$1.07 \pm 0.05$
Bremen	$6.6 \pm 4.3$	$0.81 \pm 0.04$	$-0.22 \pm 4.00$	$1.12 \pm 0.08$

- [Title Page](#)
- [Abstract](#) | [Introduction](#)
- [Conclusions](#) | [References](#)
- [Tables](#) | [Figures](#)
- [◀](#) | [▶](#)
- [◀](#) | [▶](#)
- [Back](#) | [Close](#)
- [Full Screen / Esc](#)
- [Printer-friendly Version](#)
- [Interactive Discussion](#)



## Covariation of $X_{\text{CO}_2}$ with boreal temperature

D. Wunch et al.

**Table 5.** Slopes of  $\Delta X_{\text{CO}_2} - \delta T$  relationship in  $\text{ppm K}^{-1}$  calculated from the TCCON measurements and the model runs. The errors are the standard errors on the linear fits.

Site	TCCON	SiB	SiB 2009	CarbonTracker
Park Falls	$1.60 \pm 0.92$	$1.59 \pm 1.16$	$0.91 \pm 1.13$	$1.45 \pm 0.99$
Lamont	$1.50 \pm 1.11$	$1.18 \pm 0.53$	$0.77 \pm 0.53$	$0.92 \pm 0.67$
Bremen	$0.51 \pm 1.39$	$-0.11 \pm 1.03$	$-0.40 \pm 1.10$	$0.35 \pm 0.71$
Białystok	$1.25 \pm 2.06$	$0.71 \pm 1.72$	$-0.05 \pm 1.62$	$0.69 \pm 0.70$
Weighted Mean	$1.27 \pm 0.72$	$0.91 \pm 0.59$	$0.43 \pm 0.58$	$0.81 \pm 0.39$
Weighted Mean without Bremen	$1.49 \pm 0.84$	$1.21 \pm 0.71$	$0.66 \pm 0.68$	$0.97 \pm 0.46$

- [Title Page](#)
- [Abstract](#) | [Introduction](#)
- [Conclusions](#) | [References](#)
- [Tables](#) | [Figures](#)
- [◀](#) | [▶](#)
- [◀](#) | [▶](#)
- [Back](#) | [Close](#)
- [Full Screen / Esc](#)
- [Printer-friendly Version](#)
- [Interactive Discussion](#)



**Covariation of  $X_{CO_2}$  with boreal temperature**

D. Wunch et al.

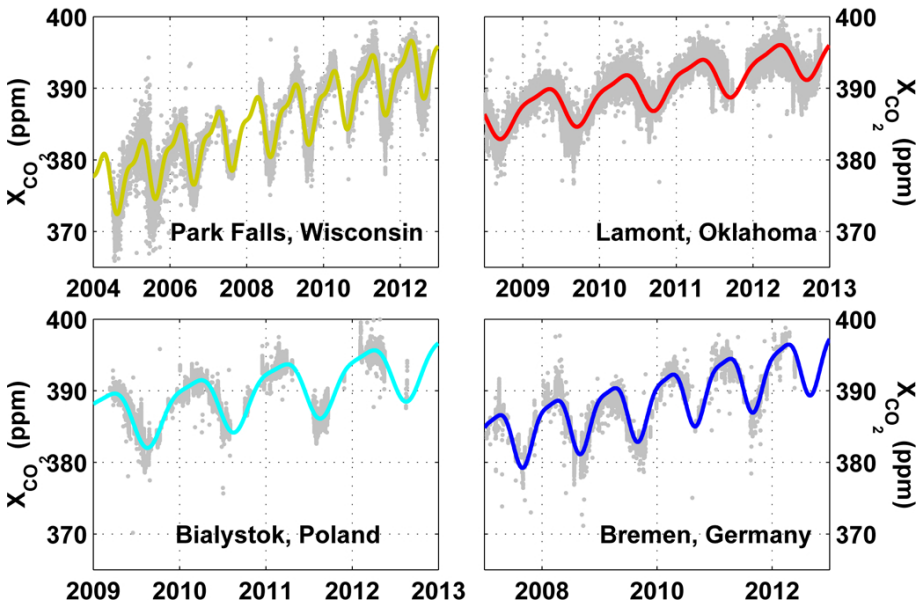
**Table 6.** The contribution of the four modules (fire, fossil fuel, terrestrial biosphere, and ocean) to the total interannual variability in CT2011. The total interannual variability (IAV) is the standard deviation of the drawdown period  $CTX_{CO_2}$  (in ppm), broken down into the fraction of that variability caused by the four modules (in percent).

Site	Total IAV (ppm)	Fires %	Fossil Fuel %	Biosphere %	Ocean %
Park Falls	0.90	6	10	82	3
Lamont	0.77	6	23	68	3
Bremen	0.48	13	22	60	5
Białystok	0.55	11	23	63	4

[Title Page](#)[Abstract](#)[Introduction](#)[Conclusions](#)[References](#)[Tables](#)[Figures](#)[|◀](#)[▶|](#)[◀](#)[▶](#)[Back](#)[Close](#)[Full Screen / Esc](#)[Printer-friendly Version](#)[Interactive Discussion](#)

**Covariation of  $X_{\text{CO}_2}$  with boreal temperature**

D. Wunch et al.

[Title Page](#)[Abstract](#)[Introduction](#)[Conclusions](#)[References](#)[Tables](#)[Figures](#)[|](#)[|](#)[Back](#)[Close](#)[Full Screen / Esc](#)[Printer-friendly Version](#)[Interactive Discussion](#)

**Fig. 1.** The time series of  $X_{\text{CO}_2}$  measured at four Northern Hemisphere TCCON stations. The solid lines are the periodic fits to the time series.

**Covariation of  $X_{\text{CO}_2}$  with boreal temperature**

D. Wunch et al.

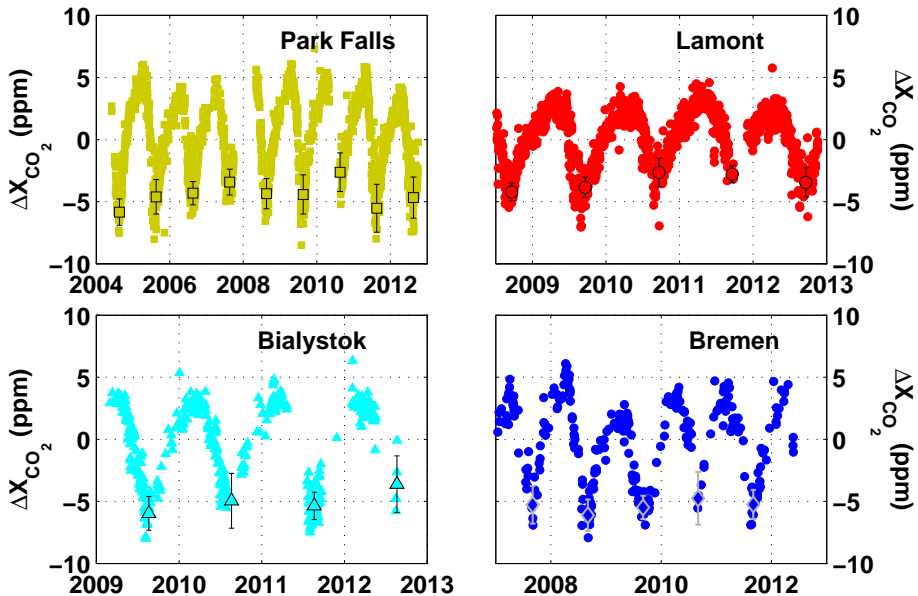


**Fig. 2.** The time series in Fig. 1 detrended to show the seasonal cycle in  $\Delta X_{\text{CO}_2}$ . The symbols show the drawdown values and their  $1 - \sigma$  errorbars. The 2007 and 2010  $\Delta X_{\text{CO}_2}$  seasonal cycle minima are relatively weak compared with those in 2008 and 2009.

**Covariation of  $X_{\text{CO}_2}$  with boreal temperature**

D. Wunch et al.

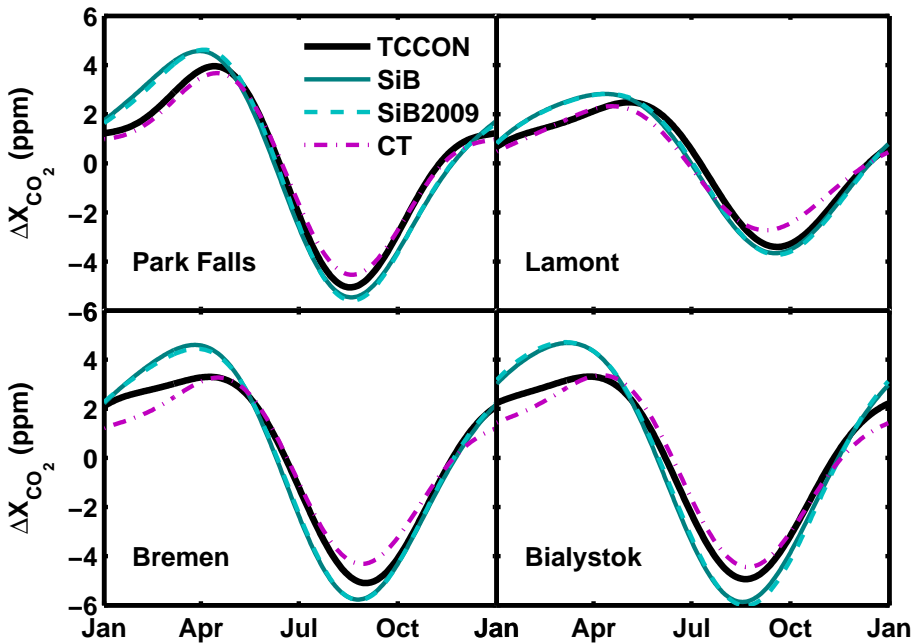


**Fig. 3.** Detrended seasonal cycles calculated by fitting the data and models (Eq. 2). Model seasonal cycles agree reasonably well with the TCCON data. See Table 4 for the amplitude ratios and time lags.

- [Title Page](#)
- [Abstract](#) [Introduction](#)
- [Conclusions](#) [References](#)
- [Tables](#) [Figures](#)
- [◀](#) [▶](#)
- [◀](#) [▶](#)
- [Back](#) [Close](#)
- [Full Screen / Esc](#)
- [Printer-friendly Version](#)
- [Interactive Discussion](#)

**Covariation of  $X_{CO_2}$  with boreal temperature**

D. Wunch et al.

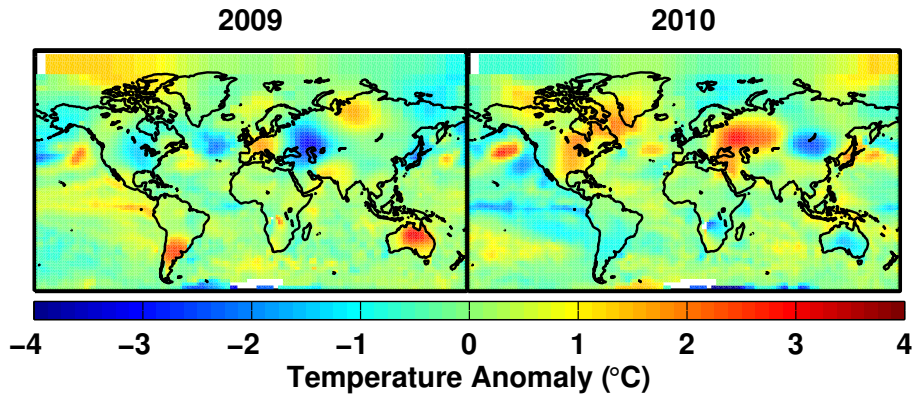


**Fig. 4.** The August surface temperature anomalies from GISS for 2009 (left) and 2010 (right) in degrees Celsius. The Northern Hemisphere 2010 temperatures are significantly warmer than those in 2009.

[Title Page](#)[Abstract](#)[Introduction](#)[Conclusions](#)[References](#)[Tables](#)[Figures](#)[|◀](#)[▶|](#)[◀](#)[▶|](#)[Back](#)[Close](#)[Full Screen / Esc](#)[Printer-friendly Version](#)[Interactive Discussion](#)

## Covariation of $X_{\text{CO}_2}$ with boreal temperature

D. Wunch et al.

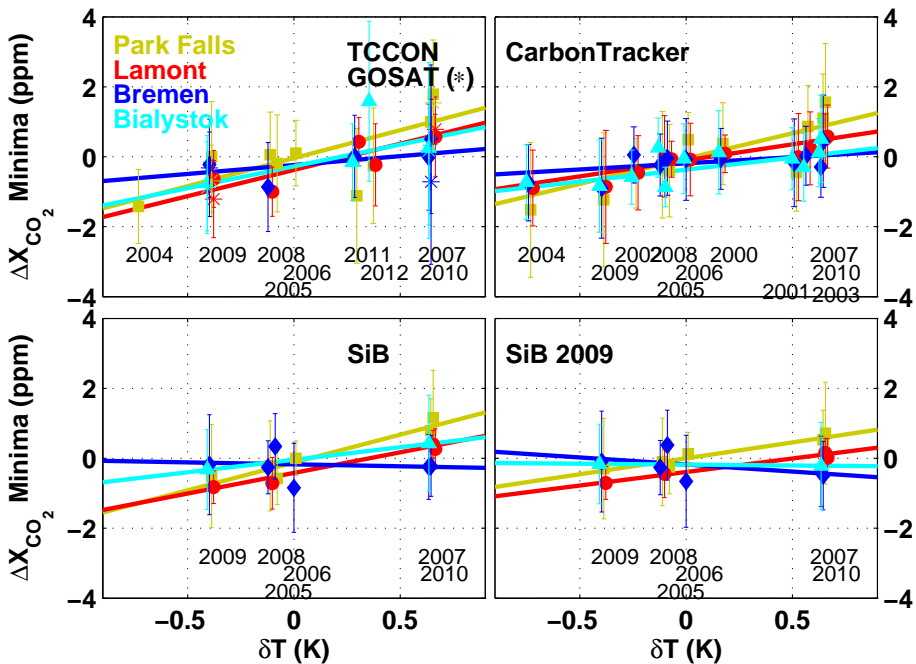


**Fig. 5.** The  $X_{\text{CO}_2}$  seasonal cycle minima plotted against the respiration-weighted surface temperature anomalies. The TCCON (symbols) and GOSAT (stars) data are plotted in the top-left panel. The remaining panels show the CarbonTracker2011 model, and the SiB model with year-specific biospheric parameters (SiB) and with a static 2009 biosphere (SiB 2009).

**Covariation of  $X_{\text{CO}_2}$  with boreal temperature**

D. Wunch et al.

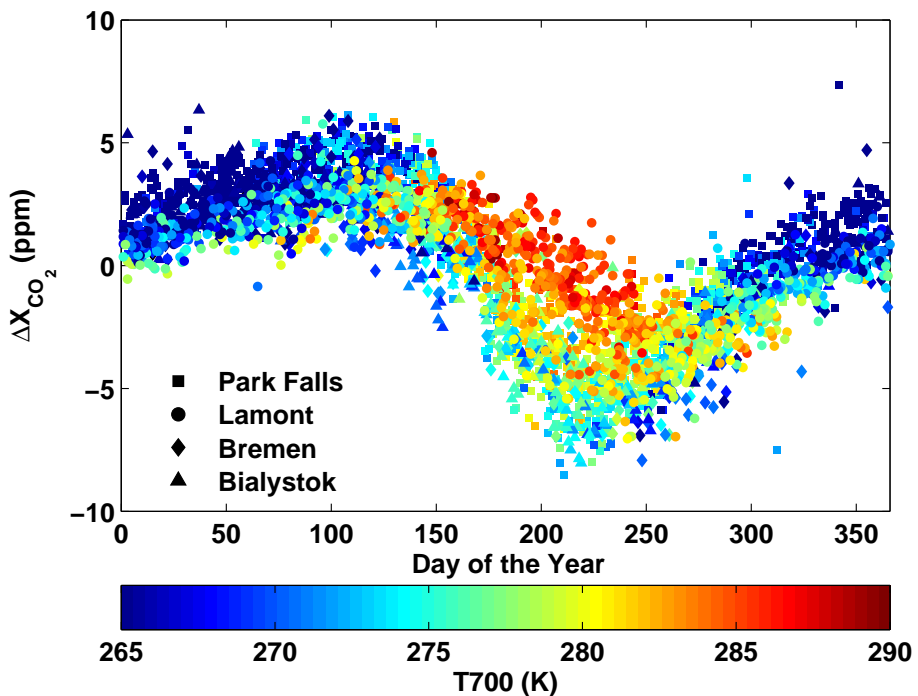


**Fig. 6.** Detrended  $X_{\text{CO}_2}$  seasonal cycles measured at the four TCCON stations. The colours are the free-troposphere temperatures (at 700 hPa, denoted T700). The colour bar is scaled to emphasize the spring and summer months. The summertime  $\Delta X_{\text{CO}_2}$  is lowest when the T700 values are coolest, and highest when the T700 values are warmest.

## Covariation of $X_{CO_2}$ with boreal temperature

D. Wunch et al.

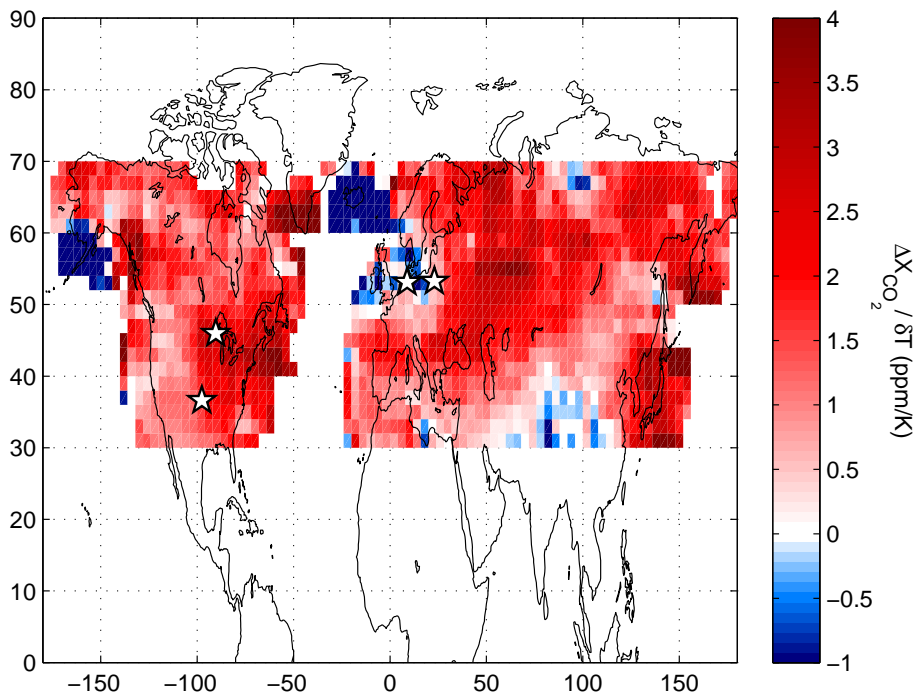


**Fig. 7.** A map of the mean  $\Delta X_{\text{CO}_2} - \delta T$  slope over the 30–70° N region from two summertime drawdown periods using GOSAT data. The TCCON stations involved in this study are indicated with white-filled black stars.

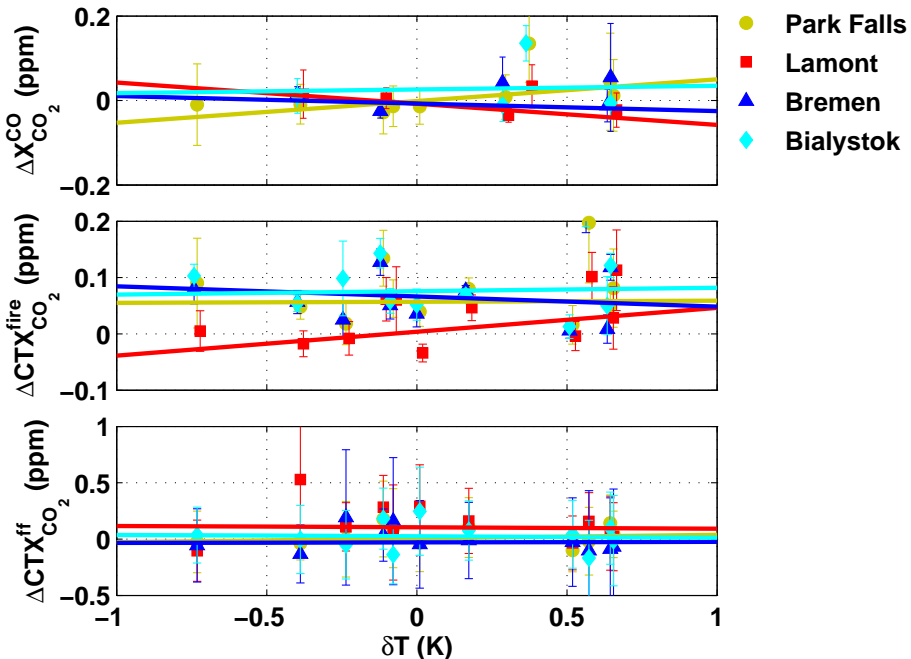


**Fig. 8.** The top panel shows the TCCON  $\Delta X_{\text{CO}_2}$  calculated from measured  $\Delta X_{\text{CO}}$  during the summertime drawdown against the respiration-weighted surface temperature, to probe the effects of forest fires on the  $\Delta X_{\text{CO}_2}$ . The solid lines show the best-fit lines, which have very poor fit statistics ( $R^2 < 0.2$ ). The middle panel shows the CT2011 fire contribution to the summertime drawdown in  $\Delta X_{\text{CO}_2}$ , which also has a negligible relationship with the respiration-weighted surface temperature. The bottom panel shows the CT2011 fossil fuel contribution to the summertime drawdown, which has a negligible relationship with the respiration-weighted surface temperature.

## Covariation of $X_{CO_2}$ with boreal temperature

D. Wunch et al.

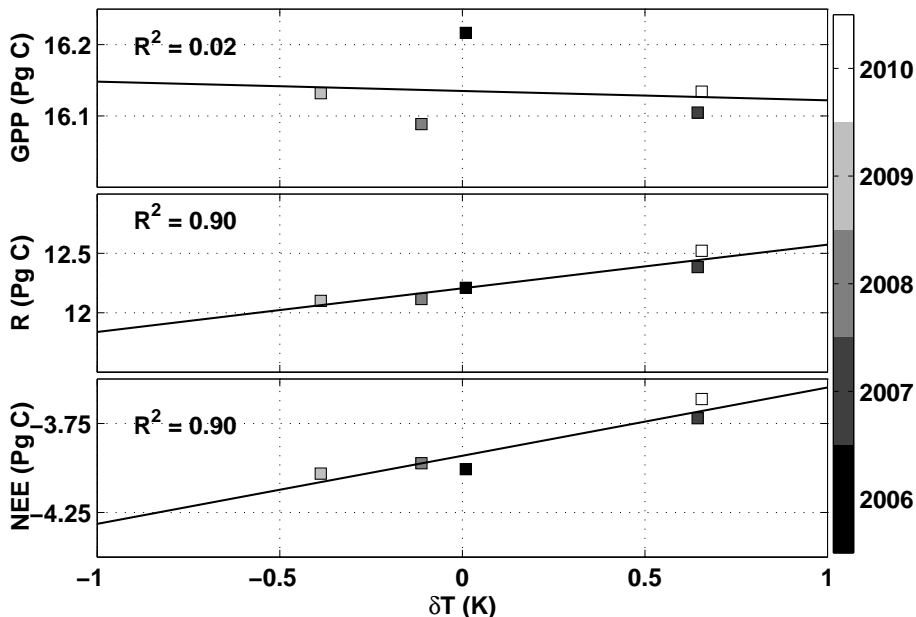


**Fig. 9.** The SiB 2006–2010 GPP (top), ecosystem respiration (middle) and NEE (bottom) integrated over the growing season (June, July and August) and over the northern midlatitudes ( $30^\circ N$ – $60^\circ N$ ), plotted as a function of the respiration-weighted surface temperature anomaly. The shades of grey indicate different years. The respiration and NEE fields have the most significant correlation with respiration-weighted temperature. The GPP does not have a significant correlation.

- [Title Page](#)
- [Abstract](#) | [Introduction](#)
- [Conclusions](#) | [References](#)
- [Tables](#) | [Figures](#)
- [◀](#) | [▶](#)
- [◀](#) | [▶](#)
- [Back](#) | [Close](#)
- [Full Screen / Esc](#)
- [Printer-friendly Version](#)
- [Interactive Discussion](#)